

3 Joint Center for Translational Medicine<sup>1</sup>, Dalian Institute of Chemical Physics Chinese Academy of Sciences<sup>2</sup>, The first Affiliated Hospital of Liaoning Medical University<sup>3</sup>, No. 457, Zhongshan Road, Dalian 116023, China

## Arbidol exhibits strong inhibition towards UDP-glucuronosyltransferase (UGT) 1A9 and 2B7

XIN LIU<sup>1</sup>, TING HUANG<sup>2</sup>, JIAN-XING CHEN<sup>2</sup>, JIA ZENG<sup>2</sup>, XU-RAN FAN<sup>3</sup>, XU-ZHU<sup>3</sup>, ZHEN-WEN YU<sup>3</sup>, XIAO-YU SUN<sup>3</sup>, MO HONG<sup>3</sup>, HONG-ZHI SUN<sup>1</sup>

Received May 10, 2012, accepted June 22, 2012

Hong-Zhi Sun, The First Affiliated Hospital of Liaoning Medical University, Jinzhou, 121001, China  
cmushz@163.com

Pharmazie 68: 945–950 (2013)

doi: 10.1691/ph.2013.2641

The aim of the present study was to investigate arbidol's inhibition towards UDP-glucuronosyltransferase (UGT) 1A9 and 2B7. The nonspecific probe substrate 4-methylumbelliferone (4-MU) and recombinant UGT enzymes (UGT1A9, UGT2B7) were firstly used to evaluate the inhibition of arbidol towards UGT1A9 and UGT2B7. Furthermore, specific substrates of UGT1A9 and UGT2B7 propofol and zidovudine (AZT) were used to determine the inhibition of arbidol towards UGT1A9 and UGT2B7. Inhibition type and inhibition kinetic parameters ( $K_i$ ) were determined. *In vitro-in vivo* extrapolation (IV-IVE) was performed to predict *in vivo* DDI magnitude induced by arbidol. Arbidol was demonstrated to exhibit competitive inhibition towards UGT1A9 and UGT2B7 without substrate-dependent behaviour. The inhibition kinetic parameters ( $K_i$ ) were calculated to be 0.5  $\mu\text{M}$ , 3.5  $\mu\text{M}$ , 2.8  $\mu\text{M}$ , 29.7  $\mu\text{M}$  for UGT2B7-mediated 4-MU glucuronidation, UGT1A9-mediated 4-MU glucuronidation, UGT2B7-mediated AZT glucuronidation, and UGT1A9-mediated propofol glucuronidation, respectively. Using these parameters, the *in vivo* alteration of area under of concentration-time curve (AUC) was calculated to be 156%, 22%, 28% and 2.6%, respectively. Given that arbidol exhibits strong inhibition towards UGT1A9 and UGT2B7, clinical monitoring should be given when arbidol was co-administered with drugs mainly undergoing UGT1A9, UGT2B7-mediated metabolism.

### 1. Introduction

Knowledge about the metabolism of a new chemical entity (NCE) is important to determine the optimal window between the drug safety parameters and its therapeutic potential (Lin and Lu 1997). Metabolic reaction of drugs is mainly catalyzed by drug metabolizing enzymes (DMEs) in the liver or other organs. When the activities of these DMEs are inhibited, the metabolic and pharmacokinetic behaviour of drugs will be influenced, which might induce severe clinical drug-drug interaction (DDIs) (Fang et al. 2011a). Cytochrome P450 (CYP)-mediated DDIs have received much attention because CYP is the most important DME and involved in the metabolism of most drugs used in clinical practice. Many *in vitro* evaluation systems have been developed to predict the *in vivo* DDI situation, and many successful examples have been reported (Fang et al. 2010, 2011b; Qu et al. 2011).

The human uridine glucuronosyltransferases (UGTs) are membrane proteins of the endoplasmic reticulum and can conjugate various endogenous substances and exogenous compounds (Miners and Mackenzie 1991). Glucuronidation reactions catalyzed by UGTs account for >35% of all phase II drug metabolism (Kiang et al. 2005). UGTs-mediated metabolisms are normally regarded as detoxifying processes, and glucuronides have greater polarity than the parent drugs. Nevertheless, some glucuronides have been reported to show pharmacological and toxicological effects (Ritter 2000). Because UGTs can conjugate a number of important endogenous sub-

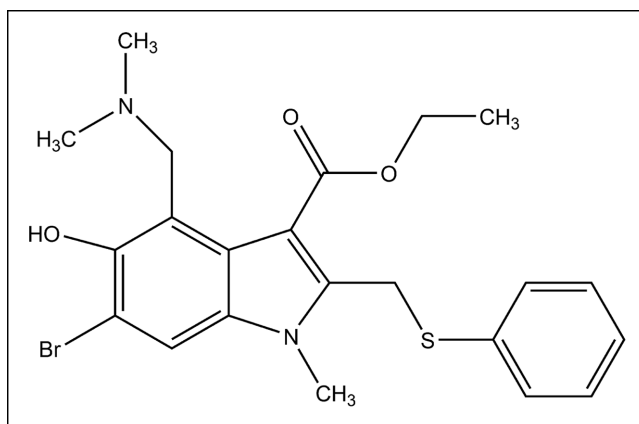


Fig. 1: The structure of arbidol.

stances (e.g. bilirubin, steroid hormones, thyroid hormones, bile acids, fat-soluble vitamins, etc.), inhibition of UGT by xenobiotics can induce not only serious DDIs but also metabolic disorders of endogenous substances.

Arbidol, ethyl-6-bromo-4-[(dimethylamino)-methyl]-5-hydroxy-1-methyl-2-[(phenylthio) methyl]-indole-3-carboxylate (Fig. 1), is an antiviral drug developed by the Chemical Drug Center of All Russian Research Institute of Pharmaceutical Chemistry together with the Institute of Medical Radiology. It has been demonstrated to exhibit inhibitory activity towards

various types of viruses, such as influenza virus, respiratory syncytial virus, adenovirus, rhinovirus, parainfluenza virus, hepatitis B virus, hepatitis C virus and coxsackie virus (Pecheu et al. 2007; Zhong et al. 2009). Therefore, arbidol is regarded as a broad-spectrum antiviral compound. Recently, arbidol has been approved for treatment of influenza in Russia, China and some European countries.

Patients often take multiple antiviral drugs and other drugs, so the DDIs associated with antiviral drugs should be considered in addition to individual drug clinical benefits and safety profiles (Taburet and Singlas 1996). The aim of the present study is to investigate the inhibitory potential of arbidol towards two important UGT isoforms: UGT1A9 and UGT2B7. Furthermore, *in vitro-in vivo* extrapolation (IV-IVE) will be carried out to predict *in vivo* DDI magnitude.

## 2. Investigations and results

### 2.1. Inhibition of UGT1A9 and UGT2B7 catalyzed 4-MU glucuronidation by arbidol

Arbidol strongly inhibited UGT2B7 and UGT1A9-mediated 4-MU glucuronidation in a concentration-dependent manner (Fig. 2A and Fig. 3A). Both Dixon and Lineweaver-Burk plots showed that both the inhibition of UGT2B7 (Fig. 2B and Fig. 3B) and UGT1A9 (Fig. 2C and Fig. 3C) were best fit to the competi-

tive inhibition type. The reversible inhibition kinetic parameters ( $K_i$ ) were calculated to be  $0.5 \mu\text{M}$  and  $3.5 \mu\text{M}$  for UGT2B7 and UGT1A9, respectively.

### 2.2. Arbidol inhibited UGT1A9-mediated propofol glucuronidation

Arbidol was demonstrated to inhibit UGT1A9-mediated glucuronidation of propofol in a concentration-dependent manner (Fig. 4A). Dixon (Fig. 4B) and Lineweaver-Burk (Fig. 4C) plots showed the inhibition behaviour was best fit to the competitive type, and the  $K_i$  value was determined to be  $29.7 \mu\text{M}$  (Fig. 4D).

### 2.3. Investigation of the inhibitory potential of arbidol towards glucuronidation of AZT

Arbidol showed a concentration-dependent inhibition towards UGT1A9-mediated glucuronidation of AZT (Fig. 5A). Dixon (Fig. 5B) and Lineweaver-Burk (Fig. 5C) plots showed the inhibition behaviour was best fit to the competitive type, and the  $K_i$  value was determined to be  $2.8 \mu\text{M}$  (Fig. 4D).

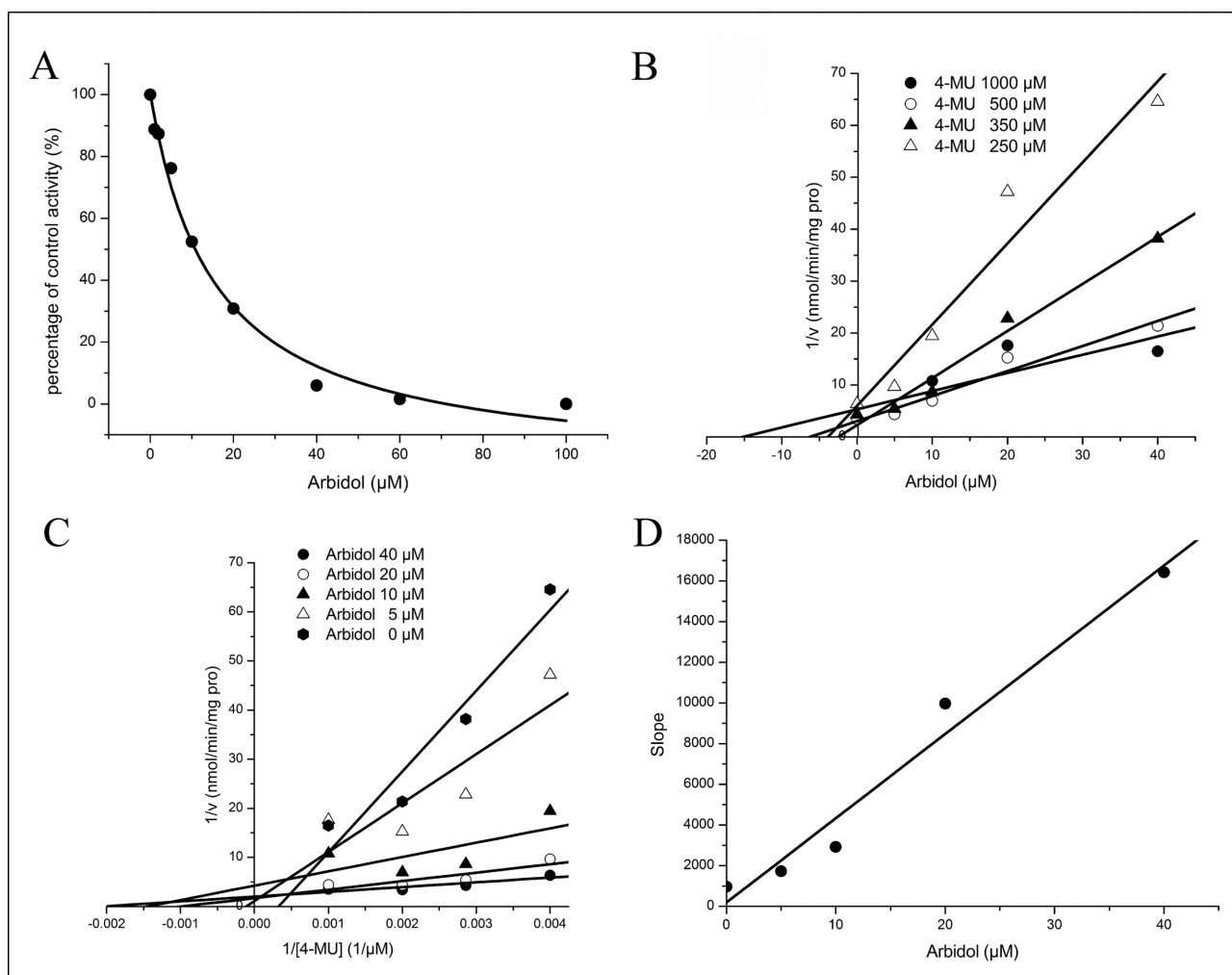


Fig. 2: Reversible inhibition of recombinant UGT2B7-mediated 4-MU glucuronidation by arbidol. (A) Inhibitory potential of arbidol on 4-MU glucuronidation activity. (B) Lineweaver-Burk plot of inhibitory effects of arbidol on 4-MU glucuronidation activity. (C) Dixon plot of inhibitory effects of arbidol on 4-MU glucuronidation activity. (D) Second plot of slopes from Lineweaver-Burk plot vs. arbidol concentrations.

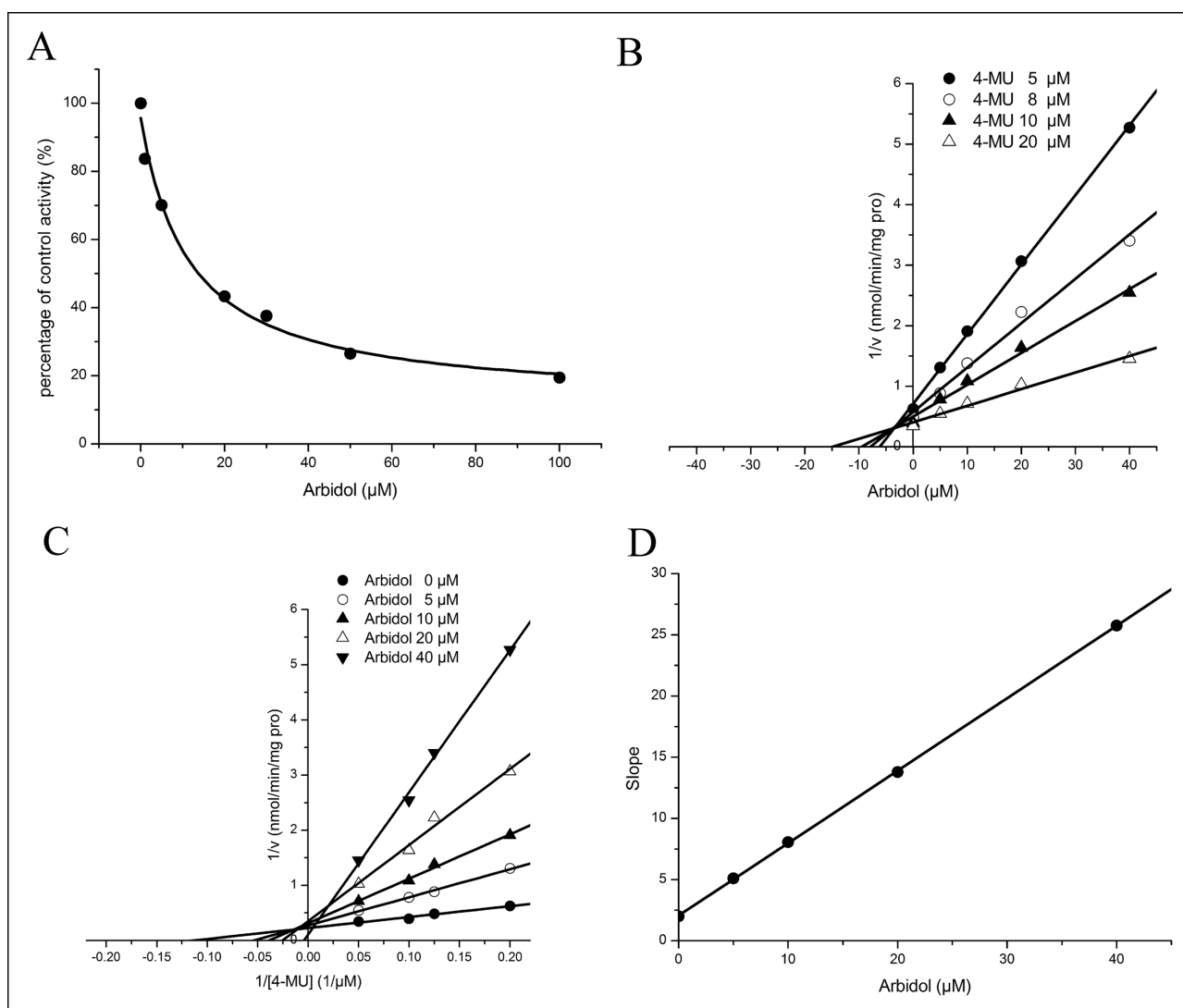


Fig. 3: Reversible inhibition of recombinant UGT1A9-mediated 4-MU glucuronidation by arbidol. (A) Inhibitory potential of arbidol on 4-MU glucuronidation activity. (C) Dixon plot of inhibitory effects of arbidol on 4-MU glucuronidation activity. (B) Lineweaver-Burk plot of inhibitory effects of arbidol on 4-MU glucuronidation activity. (D) Second plot of slopes from Lineweaver-Burk plot vs. arbidol concentrations.

#### 2.4. Prediction of *in vivo* DDI magnitude

The maximum plasma drug concentration ( $C_{\text{max}}$ ) of arbidol has been reported to be 414.8 ng/ml (0.78  $\mu\text{M}$ ) (Liu et al. 2009). Using  $C_{\text{max}}$  as the value of  $[I]$ , the ratio of  $\text{AUC}_i/\text{AUC}$  was calculated to be 2.56, 1.22, 1.28, 1.026 when using the  $K_i$  value of 0.5  $\mu\text{M}$ , 3.5  $\mu\text{M}$ , 2.8  $\mu\text{M}$  and 29.7  $\mu\text{M}$ , respectively.

### 3. Discussion

UGT1A9 and UGT2B7 are the most important UGT isoforms. UGT1A9 has been demonstrated to be involved in the metabolism of endogenous estrogenic and thyroid hormones, as well as a variety of drugs, such as acetaminophen (Court et al. 2001), diclofenac (King et al. 2001), propofol (Soars et al. 2003), and mycophenolic acid (Bernard and Guillemette 2004). UGT2B7 has been reported to catalyze many important clinical drugs, including the antiretroviral drug zidovudine (AZT). Inhibition of the activity of these two UGT isoforms might change the pharmacokinetic behaviour of drugs mainly undergoing UGT1A9, UGT2B7-mediated glucuronidation, which will result in serious DDIs and adverse reactions. For example, the direct inhibition of UDP-glucuronosyltransferase activities has been identified as a mechanism of potentiation of acetaminophen

hepatotoxicity. Fluconazole could increase the AUC,  $C_{\text{max}}$  and  $t_{1/2}$  of AZT through inhibition of AZT glucuronidation, which is demonstrated by the reduction of formation of AZT glucuronide and the urinary molar ratio of AZT glucuronide to AZT (Sahai et al. 1994).

In the present study attention was paid to the evaluation of inhibitory potential of arbidol towards UGT1A9 and UGT2B7. Different enzyme source and substrates might significantly influence the inhibition of compounds towards DMEs. The experiment carried out by Dong et al. (2011) showed that the inhibition of CYP3A by erlotinib exhibited substrate-dependent behaviour. When probe substrate of CYP3A testosterone was replaced with nifedipine, the inhibition type changed from competitive inhibition to noncompetitive inhibition (Jin et al. 2011). Therefore, three different substrates were selected to evaluate the inhibitory potential of arbidol towards UGT1A9 and UGT2B7, including a non-specific substrate 4-MU, and the specific substrates of UGT1A9 and UGT2B7 propofol and AZT. The corresponding enzyme sources were recombinant UGT isoforms and human liver microsomes. Arbidol was demonstrated to exhibit competitive inhibition towards both UGT1A9 and UGT2B7.

The *in vivo* DDI magnitude was influenced by both inhibitory capacity of inhibitor and *in vivo* plasma concentration of inhibitor. Therefore, *in vitro-in vivo* extrapolation (IV-IVE) was

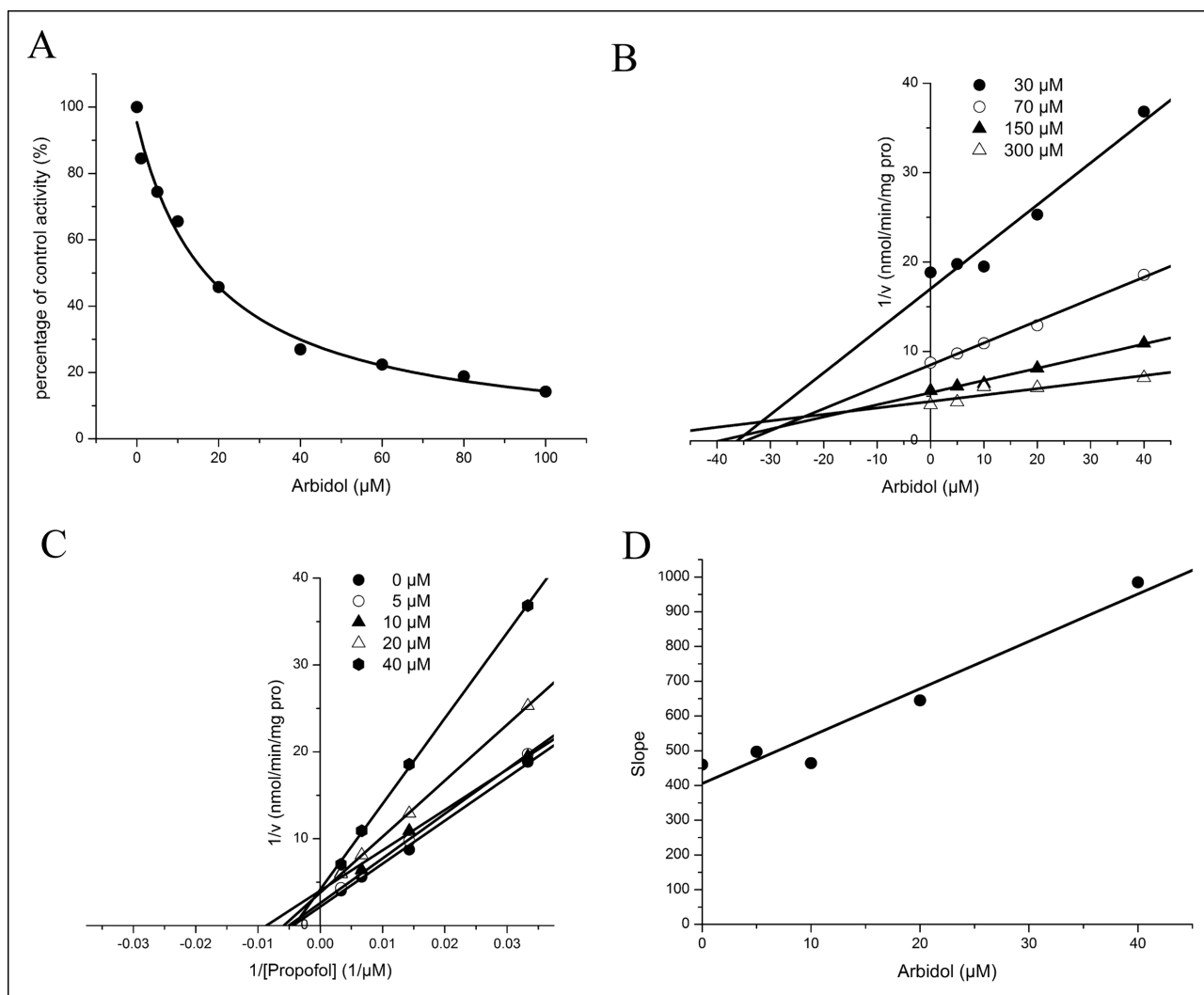


Fig. 4: Reversible inhibition of UGT1A9-mediated propofol glucuronidation reaction. (A) Inhibitory potential of arbidol on propofol glucuronidation activity. (B) Lineweaver-Burk plot of inhibitory effects of arbidol on propofol glucuronidation activity. (C) Dixon plot of inhibitory effects of arbidol on propofol glucuronidation activity. (D) Second plot of slopes from Lineweaver-Burk plot vs. arbidol concentrations.

further performed using the maximum plasma concentration of arbidol, and the AUC alteration of co-administered drugs was calculated to be 156%, 28% for UGT2B7-mediated metabolism when using 4-MU and AZT as probe substrates, respectively. The change of AUC of co-administered drugs was 22% and 2.6% for UGT1A9-catalyzed metabolism when utilizing 4-MU and propofol as probe substrates, respectively.

In conclusion, the combination of arbidol with other drugs might result in DDIs with drugs mainly undergoing UGT1A9 and UGT2B7-mediated metabolism. Therefore, clinical monitoring is needed when using arbidol.

## 4. Experimental

### 4.1. Reagents

Arbidol hydrochloride (purity > 98%) was obtained from the National Institute for the Control of Pharmaceutical and Biological Products, Beijing, People's Republic of China. 7-hydroxycoumarin, propofol, zidovudine (AZT), 4-methylumbelliferone (4-MU), 4-methylumbelliferone- $\beta$ -D-glucuronide (4-MUG), alamethicin, magnesium chloride ( $\text{MgCl}_2$ ), D-saccharic acid 1, 4-lactone, UDP-glucuronic acid trisodium salt (UDPGA) were purchased from Sigma-Aldrich (St. Louis, MO). All other reagents were of HPLC grade or of the highest grade commercially available.

Human liver samples were obtained from Dalian Medical University (Dalian, Liaoning province, China) with the approval of the local ethics committee at the university. Any information on the medication history of the samples is not gained. A panel of human liver microsomes (HLMs) was pre-

pared from twelve liver samples obtained from male and female patients by differential ultracentrifugation as described previously (Sun et al. 2010a, b). Microsomal protein concentrations were determined by the Lowry method with bovine serum albumin as standard (Lowry et al. 1951). Recombinant human UGT supersomes UGT1A9 and UGT2B7 expressed in baculovirus-infected insect cells were purchased from BD Gentest Corp. (Woburn, MA, USA).

### 4.2. Inhibition of 4-MU glucuronidation

The probe substrate for all tested UGT isoforms was 4-MU which is a non-selective substrate of UGTs. Incubations with each UGT isoform were carried out as reported previously (Huang et al. 2010, 2011; Dong et al. 2012). The mixture (200  $\mu\text{L}$  total volume) contained 0.05 mg/ml of recombinant UGT1A9 and UGT2B7, 5 mM UDPGA, 5 mM  $\text{MgCl}_2$ , 50 mM Tris-HCl buffer (pH 7.4) and 4-MU in the absence or presence of different concentrations of arbidol. The concentrations of 4-MU were 30  $\mu\text{M}$  and 350  $\mu\text{M}$  for UGT1A9 and UGT2B7, respectively. Arbidol was dissolved in methanol and the final concentration of methanol was 0.5% (v/v). After 5 min pre-incubation at 37  $^\circ\text{C}$ , the UDPGA was added in the mixture to initiate the reaction. The incubation time was 120 min and 30 min for UGT2B7 and UGT1A9, respectively. The reactions were quenched by adding 100  $\mu\text{L}$  acetonitrile with 7-hydroxycoumarin (100  $\mu\text{M}$ ) as internal standard. The mixture was centrifuged at  $20000 \times g$  for 10 min and an aliquot of supernatant was transferred to an autoinjector vial for HPLC analysis. The HPLC system (Shimadzu, Kyoto, Japan) contained a SCL-10A system controller, two LC-10AT pumps, a SIL-10A auto injector, and a SPD-10AVP UV detector. Chromatographic separation was carried out using a C18 column (4.6  $\times$  200 mm, 5  $\mu\text{m}$ , Kromasil).

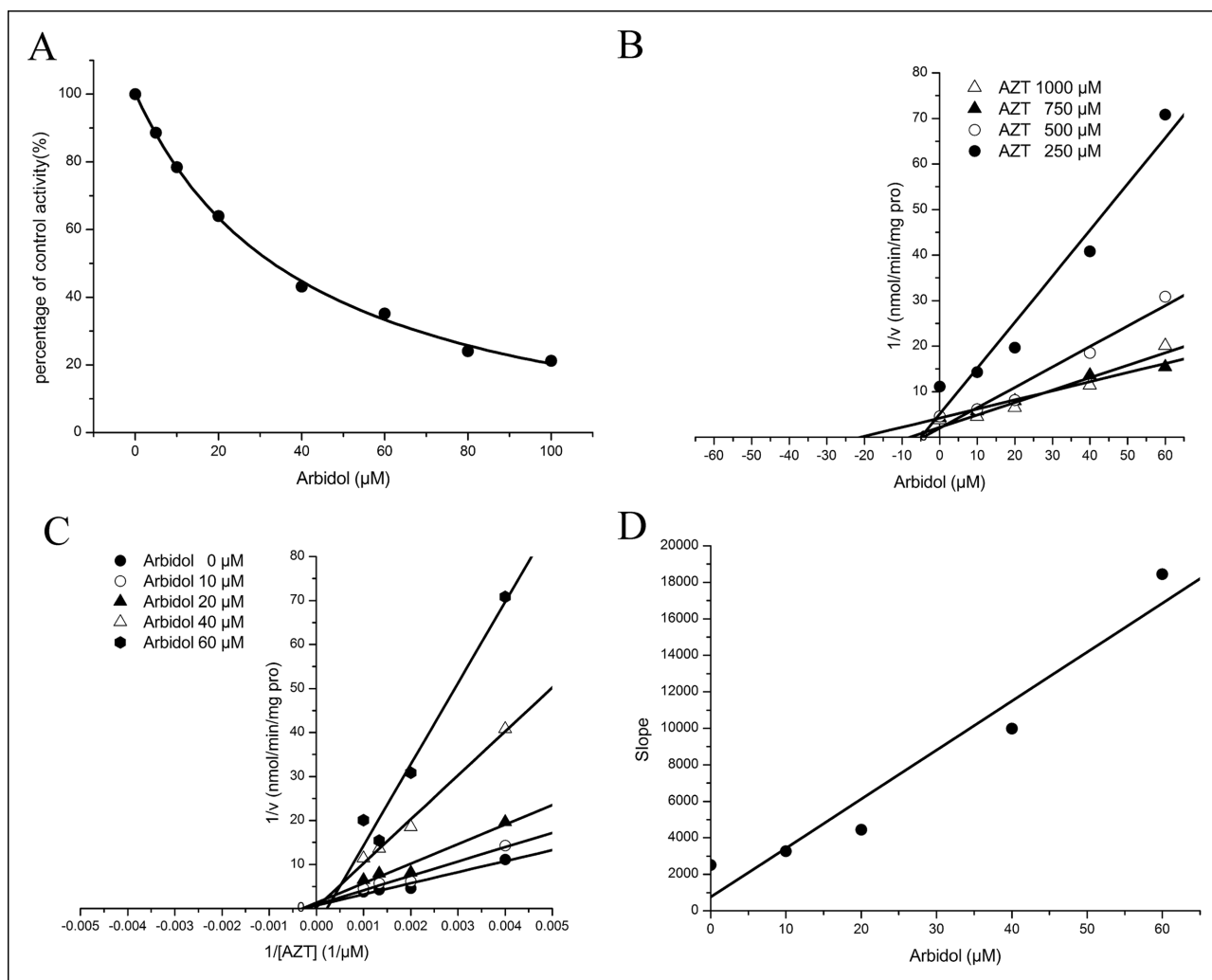


Fig. 5: Reversible inhibition of recombinant UGT2B7-mediated AZT glucuronidation by arbidol. (A) Inhibitory potential of arbidol on AZT glucuronidation activity. (B) Lineweaver-Burk plot of inhibitory effects of arbidol on AZT glucuronidation activity. (C) Dixon plot of inhibitory effects of arbidol on AZT glucuronidation activity. (D) Second plot of slopes from Lineweaver-Burk plot vs. arbidol concentrations.

#### 4.3. Inhibition of propofol glucuronidation

Propofol, mainly metabolized by UGT1A9, could be used as a probe substrate for UGT1A9 (Liang et al. 2011). A typical incubation mixture contained 0.1 mg/mL HLM, 5 mM UDPGA, 5 mM  $\text{MgCl}_2$ , 50 mM Tris-HCl buffer (pH = 7.4), 50  $\mu\text{g}/\text{mg}$  protein alamethicin and propofol (70  $\mu\text{M}$ ) in the absence or presence of different concentrations of arbidol. A Shimadzu LC/MS-2010EV mass spectrometer (Kyoto, Japan) was used to analyze the reaction mixture. It was equipped with two LC-20AD pumps, a DDU-20A3 vacuum degasser, an SIL-20A8HT autosampler, a CTO-20AC column oven, an SPD-M 20A diode array detector, a CBM-20A communications bus module and a mass detector with an ESI interface. A Shim-pack XRODS column (100 mm  $\times$  2.0 mm, 2.2  $\mu\text{m}$ , Shimadzu) was kept at 40  $^\circ\text{C}$ . The mobile phase contains acetonitrile (A) and  $\text{H}_2\text{O}$  containing 0.2% acetic acid (B). The gradient conditions were as follows: 0–2 min, 95–83% B; 2–7 min, 83–76% B; 7–9.5 min, 10% B; 9.5–12.5 min, 95% B. The flow rate was 0.3 mL/min and the injection volume was 10  $\mu\text{L}$ . The MS conditions were as follows: voltage, 4 kV; interface voltage, 40 V; nebulizing gas ( $\text{N}_2$ ) flow was 1.5 L/min and the drying gas ( $\text{N}_2$ ) pressure was set at 0.06MPa. Negative ion of [M-H]<sup>-</sup> of propofol O-glucuronide which was 353 and [M-H]<sup>-</sup> of I.S. (4-MUG) which was 351 were employed for determination with the SIM mode.

#### 4.4. Inhibition of zidovudine (AZT) glucuronidation

The glucuronidation of zidovudine (AZT) has been widely regarded as the probe substrate of UGT2B7, and the experiment was carried out as previously described (Barbier et al. 2000). In brief, a typical incubation mixture contained 0.1 mg/mL HLM, 5 mM UDPGA, 5 mM  $\text{MgCl}_2$ , 50 mM Tris-HCl buffer (pH = 7.4), 50  $\mu\text{g}/\text{mg}$  protein alamethicin and AZT (500  $\mu\text{M}$ ) in the absence or presence of different concentrations of arbidol.

#### 4.5. Determination of inhibition kinetic parameters

Inhibition kinetic parameters ( $K_i$ ) were determined utilizing various concentrations of 4-MU, propofol, or AZT in the presence of different concentrations of arbidol. Dixon and Lineweaver plots were adapted to determine the inhibition type, and second plot of slopes from Lineweaver-Burk plot vs arbidol concentrations was utilized to calculate the  $K_i$  value.

#### 4.6. In vitro-in vivo extrapolation (IV-IVE)

The equation  $\text{AUC}_i/\text{AUC} = 1 + [I]/K_i$  was employed to predict the *in vivo* DDI magnitude. The terms in the equation were defined as follows:  $\text{AUC}_i/\text{AUC}$  is the predicted ratio of *in vivo* exposure of co-administered drugs with co-administration of arbidol vs. that in control situation.  $K_i$  is the reversible inhibition constant. [I] is the *in vivo* concentration of arbidol.

#### References

- Barbier O, Turgeon D, Girard C, Green MD, Tephly TR, Hum DW, Belanger A (2000) 3'-Azido-3'-deoxythymidine (AZT) is glucuronidated by human UDP-glucuronosyltransferase 2B7 (UGT2B7). *Drug Metab Dispos* 28: 497–502.
- Bernard O, Guillemette C (2004) The main role of UGT1A9 in the hepatic metabolism of mycophenolic acid and the effects of naturally occurring variants. *Drug Metab Dispos* 32: 775–778.
- Court MH, Duan SX, von Moltke LL, Greenblatt DJ, Patten CJ, Miners JO, Mackenzie PI (2001) Interindividual variability in acetaminophen glucuronidation by human liver microsomes: identification of relevant acetaminophen UDP-glucuronosyltransferase isoforms. *J Pharmacol Exp Ther* 299: 998–1006.

- Dong PP, Fang ZZ, Zhang YY, Ge GB, Mao YX, Zhu LL, Qu YQ, Li W, Wang LM, Liu CX, Yang L (2011) Substrate-dependent modulation of the catalytic activity of CYP3A by erlotinib. *Acta Pharmacol Sin* 32: 399–407.
- Dong RH, Fang ZZ, Zhu LL, Liang SC, Ge GB, Yang L, Liu ZY (2012) Investigation of UDP-glucuronosyltransferases (UGT) inhibitory properties of carvedilol. *Phytother Res* 26: 86–90.
- Fang ZZ, Zhang YY, Ge GB, Huo H, Liang SC, Yang L (2010) Time-dependent inhibition (TDI) of CYP3A4 and CYP2C9 by nescapine potentially explains clinical nescapine-warfarin interaction. *Br J Clin Pharmacol* 69: 193–199.
- Fang ZZ, Zhang YY, Wang XL, Cao YF, Huo H, Yang L (2011a) Bioactivation of herbal constituents: simple alerts in the complex system. *Expert Opin Drug Metab Toxicol* 7: 989–1007.
- Fang ZZ, Zhang YY, Ge GB, Liang SC, Sun DX, Zhu LL, Dong PP, Cao YF, Yang L (2011b) Identification of cytochrome P450 (CYP) isoforms involved in the metabolism of corynoline, and assessment of its herb–drug interaction. *Phytother Res* 25: 256–263.
- Huang T, Fang ZZ, Yang L (2010) Strong inhibitory effect of medroxyprogesterone acetate (MPA) on UDP-glucuronosyltransferase (UGT) 2B7 might induce drug–drug interactions. *Pharmazie* 65: 919–921.
- Huang T, Fang ZZ, Zhang YY, Zhu LL, Feng LL, Zheng W, Cao YF, Sun DX, Yang L (2011) Inhibitory potential of chlormadinone acetate (CMA) on five important UDP-glucosyltransferases in human liver. *Pharmazie* 66: 212–215.
- Jin XL, Tang SH, Fang ZZ, Qu YQ, Liang R, Gao ZM, Tang B, Sun DG, Li M, Yang L, Wang LM (2011) Reversible and time-dependent inhibition of CYP3A4-mediated nifedipine oxidation by nescapine. *Lat Am J Pharm* 30: 1854–1857.
- Kiang TK, Ensom MH, Chang TK (2005) UDP-glucuronosyltransferases and clinical drug–drug interactions. *Pharmacol Ther* 106: 97–132.
- King CD, Tang W, Ngui J, Tephly T, Brau M (2001) Characterization of rat and human UDP-glucuronosyltransferases responsible for the in vitro glucuronidation of diclofenac. *Toxicol Sci* 61: 49–53.
- Liang SC, Ge GB, Liu HX, Shang HT, Wei H, Fang ZZ, Zhu LL, Mao YX, Yang L (2011) Determination of propofol UDP-glucuronosyltransferase (UGT) activities in hepatic microsomes from different species by UFLC–ESI-MS. *J Pharm Biomed Anal* 54: 236–241.
- Lin JH, Lu AYH (1997) Role of pharmacokinetics and metabolism in drug discovery and development. *Pharmacol Rev* 49: 403–449.
- Liu MY, Wang S, Yao WF, Wu HZ, Meng SN, Wei MJ (2009) Pharmacokinetic properties and bioequivalence of two formulations of arbidol: an open-label, single-dose, randomized-sequence, two-period crossover study in healthy Chinese male volunteers. *Clin Ther* 31: 784–792.
- Lowry OH, Rosebrough NJ, Farr AL, Randall RJ (1951) Protein measurement with the Folin phenol reagent. *J Biol Chem* 193: 265–275.
- Miners JO, Mackenzie PI (1991) Drug glucuronidation in human. *Pharmacol Ther* 51: 347–369.
- Pecheu EJ, Lavillette D, Alcaras F, Molle J, Boriskin YS, Roberts M, Cosset FL, Polyak SJ (2007) Biochemical mechanism of hepatitis C virus inhibition by the broad-spectrum antiviral arbidol. *Biochemistry* 46: 6050–6059.
- Qu YQ, Fang ZZ, Yang L, Zhu LL, Dong PP, Gao ZM, Liang R, Zhang YY, Ge GB, Wang LM (2011) Reversible inhibition of four important human liver cytochrome P 450 enzymes by diethylstilbestrol. *Pharmazie* 66: 216–221.
- Ritter JK (2000) Roles of glucuronidation and UDP-glucuronosyltransferases in xenobiotic bioactivation reactions. *Chem Biol Interact* 129: 171–193.
- Sahai J, Gallicano K, Pakuts A, Cameron DW (1994) Effect of fluconazole on zidovudine pharmacokinetics in patients infected with human immunodeficiency virus. *J Infect Dis* 169: 1103–1107.
- Soars MG, Ring BJ, Wrighton SA (2003) The effect of incubation conditions on the enzyme kinetics of UDP-glucuronosyltransferases. *Drug Metab Dispos* 31: 762–767.
- Sun DX, Fang ZZ, Zhang YY, Cao YF, Yang L, Yin J (2010a) Inhibitory effects of curcumenol on human liver cytochrome P450 enzymes. *Phytother Res* 24: 1213–1216.
- Sun DX, Lu CJ, Fang ZZ, Zhang YY, Cao YF, Mao YX, Zhu LL, Yin J, Yang L (2010b) Reversible inhibition of three important human liver cytochrome P450 enzymes by tiliroside. *Phytother Res* 24: 1670–1675.
- Taburet AM, Singlas E (1996) Drug interactions with antiviral drugs. *Clin Pharmacokinet* 30: 385–401.
- Zhong Q, Yang ZQ, Liu YY, Deng H, Xiao H, Shi L, He J (2009) Antiviral activity of arbidol against coxsackie virus B5 *in vitro* and *in vivo*. *Arch Virol* 154: 601–607.